

Tetrazolyl isoxazole amino acids as ionotropic glutamate receptor antagonists: Synthesis, modelling and molecular pharmacology

Bente Frølund,^{a,*} Jeremy R. Greenwood,^a Mai M. Holm,^b Jan Egebjerg,^{b,c} Ulf Madsen,^a Birgitte Nielsen,^a Hans Bräuner-Osborne,^a Tine B. Stensbøl^c and Povl Krogsgaard-Larsen^a

^aDepartment of Medicinal Chemistry, The Danish University of Pharmaceutical Sciences, 2 Universitetsparken, DK-2100 Copenhagen, Denmark

^bDepartment of Molecular Biology, University of Aarhus, DK-8000 Aarhus C, Denmark

^cDepartment of Molecular Pharmacology, H. Lundbeck A/S, DK-2500 Valby, Denmark

Received 26 January 2005; accepted 10 June 2005

Available online 25 July 2005

Abstract—Two 3-(5-tetrazolylmethoxy) analogues, **1a** and **1b**, of (*RS*)-2-amino-3-(3-hydroxy-5-methyl-4-isoxazolyl)propionic acid (AMPA), a selective AMPA receptor agonist, and (*RS*)-2-amino-3-(5-*tert*-butyl-3-hydroxy-4-isoxazolyl)propionic acid (ATPA), a GluR5-preferring agonist, were synthesized. Compounds **1a** and **1b** were pharmacologically characterized in receptor binding assays, and electrophysiologically on homomeric AMPA receptors (GluR1–4), homomeric (GluR5 and GluR6) and heteromeric (GluR6/KA2) kainic acid receptors, using two-electrode voltage-clamped *Xenopus laevis* oocytes expressing these receptors. Both analogues proved to be antagonists at all AMPA receptor subtypes, showing potencies ($K_b = 38$ – 161 μ M) similar to that of the AMPA receptor antagonist (*RS*)-2-amino-3-[3-(carboxymethoxy)-5-methyl-4-isoxazolyl]propionic acid (AMOA) ($K_b = 43$ – 76 μ M). Furthermore, the AMOA analogue, **1a**, blocked two kainic acid receptor subtypes (GluR5 and GluR6/KA2), showing sevenfold preference for GluR6/KA2 ($K_b = 19$ μ M). Unlike the iGluR antagonist (*S*)-2-amino-3-[5-*tert*-butyl-3-(phosphonomethoxy)-4-isoxazolyl]propionic acid [(*S*)-ATPO], the corresponding tetrazolyl analogue, **1b**, lacks kainic acid receptor effects. On the basis of docking to a crystal structure of the isolated extracellular ligand-binding core of the AMPA receptor subunit GluR2 and a homology model of the kainic acid receptor subunit GluR5, we were able to rationalize the observed structure–activity relationships. © 2005 Elsevier Ltd. All rights reserved.

1. Introduction

(*S*)-Glutamic acid (Glu) is the major excitatory neurotransmitter in the central nervous system (CNS) and has been implicated in a number of neurological and psychiatric diseases.^{1–3} Glu operates via two different classes of receptors, the ionotropic and metabotropic Glu receptors.⁴ Ionotropic Glu receptors (iGluRs) are subdivided according to their sensitivity to the agonists 2-amino-3-(3-hydroxy-5-methyl-4-isoxazolyl)propionic acid (AMPA), kainic acid (KA) and *N*-methyl-D-aspartic acid (NMDA). Likewise, the metabotropic Glu receptors (mGluRs) are assigned to three classes named Groups I, II and III.⁵

Subsequent to the cloning of individual subunits, the iGluRs have been found to be homo- or heteromeric assemblies that form tetrameric ion channel complexes.⁶ Those composed of GluR1–4 are activated by AMPA and are termed AMPA receptors, while KA has high affinity for KA1,2 and lower affinity for GluR5–7, which are collectively named KA receptors.^{7,8}

The pharmacology of iGluRs has been extensively characterized using a number of selective ligands. While AMPA (Fig. 1) selectively activates receptors constructed from GluR1–4⁹ and only activates GluR5 at high concentrations, the *tert*-butyl analogue of AMPA (*RS*)-2-amino-3-(5-*tert*-butyl-3-hydroxy-4-isoxazolyl)propionic acid (ATPA) exhibits strong preference for GluR5 over AMPA receptors.^{10,11} Among the group of AMPA-derived competitive iGluR antagonists, (*RS*)-2-amino-3-[3-(carboxymethoxy)-5-methyl-4-isoxazolyl]propionic acid (AMOA) selectively blocks AMPA receptors.¹² The corresponding *tert*-butyl

Keywords: Ionotropic Glu receptors; Antagonists; AMOA; Tetrazole group.

*Corresponding author. Tel.: +45 35306495; fax: +45 35306040; e-mail: bfr@dfuni.dk

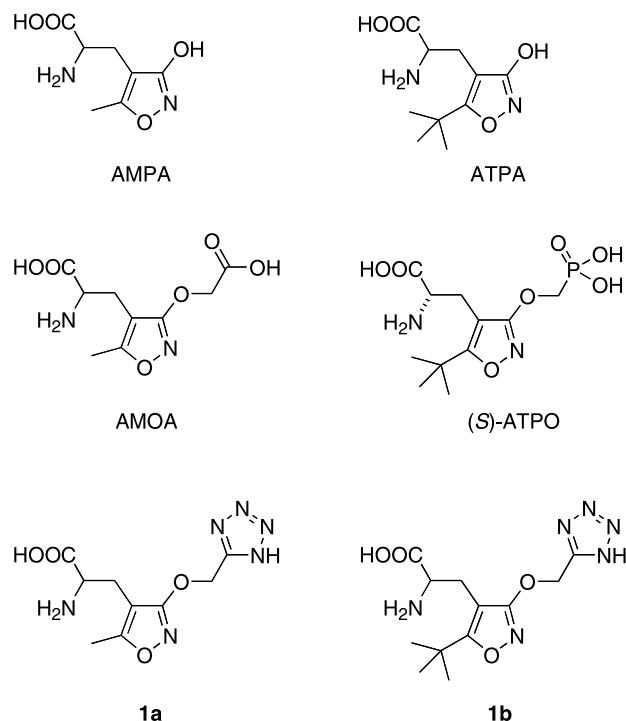


Figure 1. Structures of the iGluR agonists AMPA and ATPA, the iGluR antagonists AMOA and (*S*)-ATPO and the new tetrazolyl analogues **1a** and **1b**.

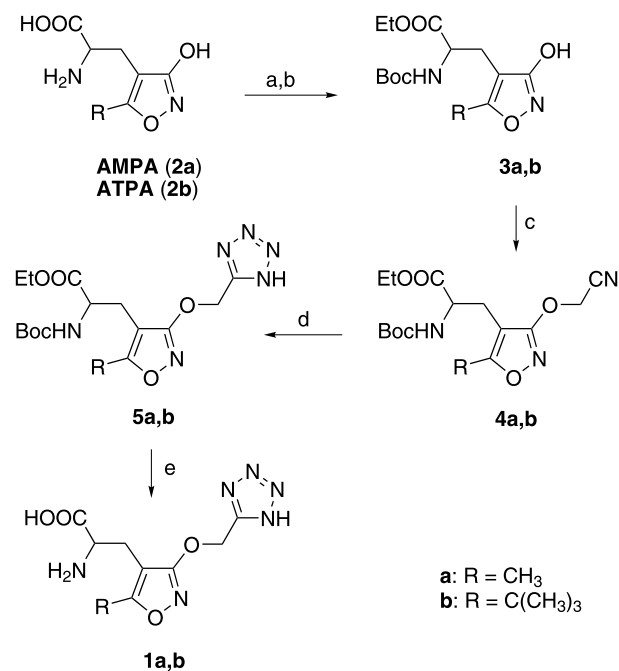
phosphono analogue (*S*)-2-amino-3-[5-*tert*-butyl-3-(phosphonomethoxy)-4-isoxazoly]propionic acid [(*S*)-ATPO] shows a markedly more potent antagonistic effect.¹³ Unlike AMOA, ATPO also antagonizes GluR5 receptors, indicating that the bulky *tert*-butyl group can be accommodated by the antagonist conformation of the GluR5 receptor complex, as shown by agonists, such as ATPA, for the activated receptor conformation.¹³

Increased lipophilicity, hydrogen bonding capability and metabolic resistance to a range of degradation pathways have made the tetrazolyl group a popular carboxyl group bioisostere in medicinal chemistry.¹⁴ In both NMDA and AMPA/KA receptor agonists and antagonists, the tetrazolyl group has been successfully used as a bioisostere for the distal carboxyl group.^{15,16} We therefore incorporated the tetrazole ring system as the distal acid in isoxazole-based AMPA/KA antagonists AMOA and (*S*)-ATPO. Here, we describe the synthesis and the pharmacological characterization of the respective tetrazolyl analogues of AMOA and (*S*)-ATPO, **1a** and **1b**. The iGluR pharmacology uncovered for these compounds are discussed on the basis of docking to experimental and homology modelled structures of iGluR ligand-binding domains.

2. Results

2.1. Chemistry

The amino acids **1a** and **1b** were prepared from the corresponding amino acids AMPA¹⁷ and ATPA,¹⁸ respec-



Scheme 1. Reagents and conditions: (a) HCl/EtOH; (b) (Boc)₂O, TFA, EtOH, 0 °C; (c) K₂CO₃, acetone then ClCH₂CN; (d) NaN₃, DMF then 2 M HCl; (e) 1 M TFA, reflux.

tively, as illustrated in Scheme 1. Initially, the amino acid moiety was protected as an ethyl ester and a *tert*-butyl carbamate (Boc) using standard procedures. Alkylation of the 3-hydroxyisoxazoles **3a** and **3b** with chloroacetonitrile under basic conditions gave the nitriles **4a** and **4b** in good yields. The tetrazole moiety was prepared by heating the corresponding nitrile with sodium azide in DMF, in the presence or absence of triethyl ammonium chloride. Compounds **5a** and **5b** were deprotected using trifluoroacetic acid, to give the free amino acids **1a** and **1b**, respectively.

2.2. In vitro pharmacology

The affinities of **1a** and **1b** for native AMPA, KA and NMDA receptors derived from rat brain synaptic membranes were determined using the radioligands [³H]AMPA, [³H]CNQX, [³H]KA and [³H]CPP (Table 1). Neither **1a** nor **1b** showed affinity (IC₅₀ >100 μM) for KA or NMDA receptors, whereas the compounds **1a** and **1b** showed micromolar affinities in the [³H]AMPA and [³H]CNQX binding assays. The observed affinities of the compounds **1a** and **1b** for AMPA receptors are similar to the affinities shown by racemic ATPO¹⁹ and AMOA.¹²

In the rat cortical wedge model,²⁰ the effects of compounds **1a** and **1b** on the depolarizations induced by AMPA (5 μM), NMDA (10 μM) and KA (5 μM) were tested (Table 1). Both **1a** and **1b** antagonized AMPA-induced depolarization with similar potencies (190 and 153 μM) slightly higher than that of AMOA (320 μM) but at higher concentrations than ATPO (28 μM). The compounds were shown to have a very weak antagonising effect on NMDA-induced depolarization, compound

Table 1. Receptor binding affinities on rat synaptic membranes and electrophysiology data from the rat cortical wedge model

	IC ₅₀ ^a (μM)				
	[³ H]AMPA	[³ H]CNQX	[³ H]KA	[³ H]CPP	Electrophysiology
AMOA ^b	90 ^c	8.0 ± 0.7	>100	>100	320 ± 25 ^d
ATPO ^b	35 ± 3	5.7 ± 3.2	>100	>100	28 ± 3 ^d
1a	17 ± 1	13.0 ± 0.6	>100	>100	190 ± 25 ^d (680 ± 100) ^e
1b	80 ± 5	16.5 ± 2.1	>100	>100	153 ± 10 ^d (24%) ^f

^a Values represent mean ± SEM, *n* = 3.^b Data from Ref. 19.^c Data from Ref. 12.^d Antagonism of 5 μM AMPA.^e Antagonism of 10 μM NMDA.^f Reduction of the response from 10 μM NMDA by 1000 μM **1b**.

1a showing an IC₅₀ of 680 μM and compound **1b** showing a 24% reduction in the response induced by 10 μM NMDA at 1 mM concentration.

Compounds **1a** and **1b** were studied for subtype selectivity using two-electrode voltage-clamped *Xenopus laevis* oocytes expressing cloned AMPA and KA receptors (Table 2 and Fig. 2). Compound **1a** showed antagonist behaviour at all AMPA receptor subtypes (GluR1–4), with *K_b* values ranging from 48 to 161 μM. In addition, compound **1a** turned out to be an antagonist at two of the KA receptor subtypes, GluR5 and GluR6/KA2, showing sevenfold preference for the GluR6/KA2 heteromers. Compound **1b** was equipotent with compound **1a** at the AMPA receptor subtypes. However, at the KA receptors GluR5 and GluR6/KA2, the potency of **1b** was greatly diminished (IC₅₀ >2.5 mM and about 800 μM, respectively).

The pharmacological effects of compounds **1a** and **1b** at mGluR1, mGluR2 and mGluR4 expressed in CHO cells, representing Groups I, II and III mGlu receptors, respectively, were tested using conventional second messenger assays. At 1 mM concentrations, no agonist or antagonist activities were observed.

2.3. Homology modelling and receptor docking

Although X-ray crystal structures for the ligand-binding domains of GluR5 and GluR6 have been solved and deposited in the Protein Data Bank (1TXF.pdb; 1S50.pdb; etc.), these are all of domain closed agonized states. Therefore, in order to probe selectivity differences

among these antagonists between AMPA and KA receptors, a homology model needed to be constructed from the domain-open state of the GluR2 ligand-binding core. ATPO, AMOA, **1a** and **1b** were docked to the experimental crystal structure of the GluR2–S1S2/ATPO complex and a modelled GluR5/ATPO complex using Glide.²⁵ The experimental and prepared positions of ATPO in GluR2 and GluR5 were returned to a fraction of an Å RMSD. The top ranked poses are depicted in Figures 3 and 4, which also show the amino acids involved in binding the ligands at each receptor. Only

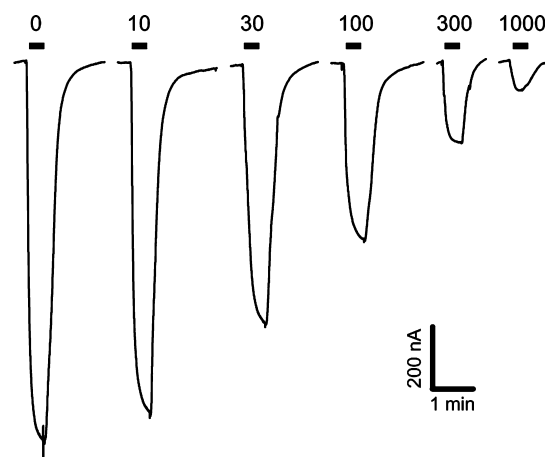


Figure 2. **1b** inhibition of 25 μM KA. The figure displays traces from a two-electrode voltage clamped *Xenopus laevis* oocyte expressing GluR2Qflop. The oocyte was clamped at −70 mV and increasing concentrations of **1b** (in μM) were added to inhibit the response elicited by 25 μM KA. The first response was elicited by KA alone.

Table 2. Electrophysiological data on oocytes expressing homomeric and heteromeric AMPA and KA receptors

	<i>K_b</i> (μM) ^a							
	GluR1	GluR1/2	GluR2Q	GluR3	GluR4	GluR5	GluR6	GluR6/KA2
AMOA	44 ^b	76 ^b	43 ± 2	NT	NT	NA ^b	NA ^b	NT
(S)-ATPO ^c	3.9	5.2	NT	15	26	24	>300	>300
1a	62 ± 13	NT	161 ± 20	48 ± 1	76 ± 4	131 ± 4	>300	19 ± 1
1b	38 ± 5	NT	96 ± 8	63 ± 2	71 ± 10	>2500	>300	≈750

NT, not tested; NA, not active.

^a Values represent mean ± SEM, *n* ≥ 3.^b Data from Ref. 28.^c Data (*K_i*) from Ref. 13.

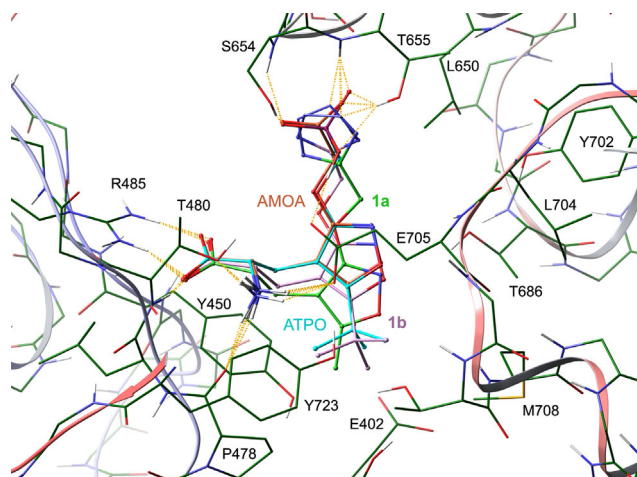


Figure 3. AMOA (orange), compounds **1a** (green) and **1b** (purple) docked into the X-ray crystal structure of the GluR2/ATPO complex.

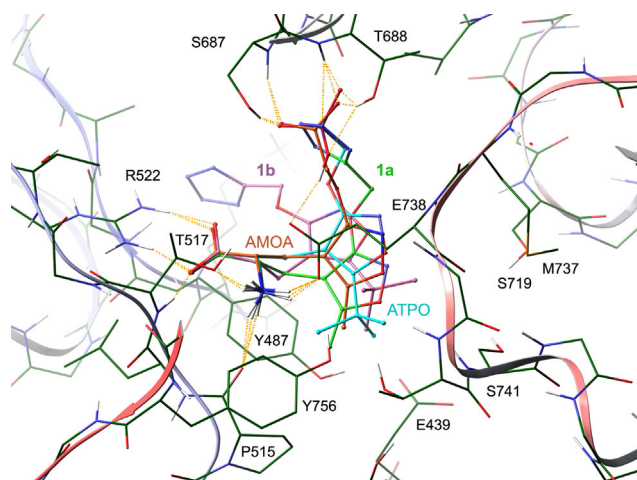


Figure 4. AMOA (orange), compounds **1a** (green) and **1b** (purple) docked into a homology model of GluR5/ATPO built from the X-ray structure of the GluR2/DNQX complex.

1b at GluR5 cannot be docked in an ATPO-like binding mode due to its size. Conversely, AMOA is too short to establish distal anion recognition at domain 2 and at the same time substantially occupies the more hydrophobic regions of the binding site closer to domain 1 of this receptor. The best poses gave Extra Precision Glidescores generally in broad qualitative agreement with experiment when converted to activities (6, 264 μ M), (5, 14 μ M), (1960, 151 μ M) and (10, 469 μ M), respectively, for AMOA, ATPO, **1a** and **1b** at (GluR2, GluR5). The rankings (ATPO > AMOA > **1b** > **1a** at GluR2 and ATPO > **1a** > AMOA > **1b** at GluR5) are in agreement with the experimental AMPA vs. GluR5 activity profiles, lending confidence in the quality of the homology model and the predicted binding modes.

3. Discussion

In the development of potent and selective ligands for iGluR receptors, the archetypal agonist AMPA that

gave name to a subclass of these receptors has been extensively used as a lead. Analogues of AMPA have been synthesized, in which the methyl group at the 5-position of the 3-isoxazolol ring has been replaced by substituents with different steric and electronic properties, providing compounds showing a variety of potencies and selectivities at AMPA and KA receptors.^{18,21–23} The results of these studies suggested that the AMPA and KA receptors may contain a cavity capable to accommodate hydrophobic substituents up to a certain size at the 5-position of the 3-isoxazolol ring of AMPA.²² On the basis of the crystal structure of the GluR2–S1S2J in complex with KA, a homology model of the activated GluR5/KA complex has been developed, and the cavity and receptor–ligand interactions studied in detail.²⁴ We now extend this approach to the antagonized state of the receptor (Figs. 3 and 4).

On the basis of a group of selective and highly potent GluR5 agonists, including ATPA, bulky substituents at the 5-position of the 3-isoxazolol ring of AMPA or at equivalent positions in analogous structures have been found to be an important structural determinant for activation of GluR5 receptors.^{25–27} Conversely, in the development of antagonists for iGluRs, the structural characteristics of the acidic moiety at the 3-position of the isoxazole ring, seem to play an important role, as exemplified by AMOA and (S)-ATPO.

In order to investigate the tetrazole ring as a bioisostere for the distal carboxyl group or phosphonic group at the 3-positions of AMOA and ATPO, respectively, we have synthesized two new potential iGluR antagonists, **1a** and **1b**. Starting from the protected AMPA and ATPA structures, the tetrazolylmethyl group was introduced, affording the desired compounds after deprotection.

The AMPA-derived antagonist AMOA, which possesses a carboxymethoxy group at the 3-position of the isoxazole ring of AMPA, is known to be a selective, but relatively weak AMPA antagonist.²⁸ In contrast to AMOA, **1a** antagonized GluR5 and GluR6/KA2 in addition to AMPA receptors. Interestingly, **1a** showed a sevenfold preference for GluR6/KA2 heteromer over GluR5.

Although (S)-ATPO is derived from the selective GluR5 agonist ATPA, it is a potent antagonist at GluR1, 20-fold more potent than AMOA,^{13,28} indicating that in addition to the space available to substituents, other factors govern the tolerance or preference for *tert*-butyl substituents in the open domain (antagonized) vs. the closed domain (agonized) AMPA and KA ligand–receptor complexes. In this study, the tetrazolylmethoxy analogue of ATPO, compound **1b**, was shown to be equipotent with ATPO as an antagonist of AMPA receptors. However, unlike the corresponding *tert*-butyl agonist ATPA and antagonist ATPO, **1b** was devoid of effect on KA receptors GluR5, GluR6, and the heteromeric GluR6/KA2 receptors. No subunit selectivity was seen for either **1a** or **1b** within the group of AMPA receptors.

To rationalize the observed structure–activity relationships, the compounds **1a**, **1b**, AMOA and ATPO were docked to a homology model of the antagonized state of GluR5 (Fig. 4). It is apparent that AMOA loses some affinity for both receptors because it fails to fill the hydrophobic cavity, while the molecule of **1b** is too long to fit into GluR5 in an ATPO-like binding mode. Binding of **1b** is conflicting with residue S741, which is most likely H-bonded to Y756 via a water molecule, and which has been shown to determine the selective activation of GluR5 by ATPA.¹¹ At AMPA receptors, compound **1b** is, however, able to fit into the slightly larger pocket known to be occupied by the *tert*-butyl group of ATPO. In general, the tetrazole anion can be considered a poorer distal carboxylate bioisostere than phosphonate at the open domain conformation of these receptors, because the geometry of this group limits the number of hydrogen bonds obtainable from the S654–T655 anion recognition site.

In conclusion, the 3-tetrazolylmethoxy analogues of AMOA and (*S*)-ATPO, **1a** and **1b**, respectively, are low-potency AMPA receptor antagonists. In addition, compound **1a** antagonizes KA receptors, showing a sevenfold preference for heteromeric GluR6/KA2 receptors over homomeric GluR5 receptors. Compound **1b** was shown to be an AMPA receptor antagonist devoid of activity at the KA receptors tested. Despite the fact that the tetrazole ring moiety generally mimics the carboxylic acid group with respect to physical and protolytic properties, the geometry of this group is not optimal for receptor recognition and blockade at these particular targets.

Despite their relatively low potency, these compounds have given further insight into structure–activity relationships for iGluR antagonists. On the basis of the selectivity profiles of compounds **1a** and **1b**, these compounds may serve as leads for the development of selective ligands for iGluR receptor subtypes in particular within the class of KA-preferring receptors.

4. Experimental

4.1. General methods

Melting points were determined in capillary tubes and are uncorrected. ¹H NMR spectra were recorded on a Bruker AC-200F (200 MHz) instrument in CDCl₃ solutions using TMS as an internal standard or in D₂O solutions using 1,4-dioxane as an internal standard. Column chromatography (CC) was performed on Merck silica gel 60 (0.06–0.200 mm). Analytical thin-layer chromatography (TLC) was carried out using Merck silica gel 60 F₂₅₄ plates. All compounds were detected as single spots on TLC plates and visualized using UV light and KMnO₄ spraying reagent. Compounds containing amino groups were also visualized using a ninhydrin spraying reagent. Elemental analyses were performed at Analytical Research Department, H. Lundbeck A/S Denmark or by Mr. J. Theiner, Department of Physical Chemistry, University of Vienna, Austria.

4.2. Ethyl (*RS*)-2-[*N*-(*tert*-butyloxycarbonyl)amino]-3-(3-hydroxy-5-methyl-4-isoxazolyl)propionate (**3a**)

Compound **2a**¹⁷ (1.18 g, 6.3 mmol) was dissolved in saturated HCl/EtOH. The reaction mixture was heated under reflux for 1.5 h. Evaporation and re-evaporation twice from toluene gave ethyl (*RS*)-2-amino-3-(3-hydroxy-5-methyl-4-isoxazolyl)propionate hydrochloride (1.48 g, 93%). To an ice-cold solution of this intermediate (1.48 g, 5.88 mmol) in EtOH (45 mL) were added TEA (2.0 mL, 14.3 mmol) and a solution of di-*tert*-butyl dicarboxylate (1.50 mL, 6.43 mmol) in EtOH (5 mL), and the mixture was stirred at 0 °C for 1.5 h. The reaction mixture was evaporated, and H₂O (40 mL) and EtOAc (50 mL) were added. The mixture was cooled on ice and acidified with AcOH. The phases were separated, and the aqueous phase was extracted with EtOAc (2 × 100 mL). The combined and dried organic phases were filtered and evaporated to give the title compound as colourless crystals (1.3 g, 42%). ¹H NMR (CDCl₃) δ 8.90 (br s, 1H), 5.50–5.32 (m, 1H), 4.55–4.38 (m, 1H), 4.28–4.05 (m, 2H), 2.87–2.72 (m, 2H), 2.23 (s, 3H), 1.40 (s, 9H), 1.22 (t, 3H, *J* = 7.0 Hz).

4.3. Ethyl (*RS*)-2-[*N*-(*tert*-butyloxycarbonyl)amino]-3-(3-hydroxy-5-*tert*-butyl-4-isoxazolyl)propionate (**3b**)

The preparation of **3b** was carried out according to the procedure for **3a** using **2b**¹⁸ (2.0 g, 8.75 mmol) to give the title compound in a total of 64% as light yellow oil. ¹H NMR (CDCl₃) δ 9.58 (br s, 1H), 5.31–5.49 (m, 1H), 4.35–4.52 (m, 1H), 4.20 (q, 2H, *J* = 7.0 Hz), 2.71–3.08 (m, 2H), 1.38 (s, 18H), 1.25 (t, 3H, *J* = 7.0 Hz).

4.4. Ethyl (*RS*)-2-[*N*-(*tert*-butyloxycarbonyl)amino]-3-[3-(cyanomethoxy)-5-methyl-4-isoxazolyl]propionate (**4a**)

A mixture of **3a** (700 mg, 2.2 mmol) and K₂CO₃ (615 mg, 4.5 mmol) in acetone (60 mL) was stirred at rt for 30 min. Chloroacetonitrile (423 μL, 6.7 mmol) was slowly added and stirring was continued for 18 h at 50 °C. After cooling, the reaction mixture was filtered and evaporated. CC [toluene–EtOAc (1:1)] gave **4a** (560 mg, 71%) as viscous yellow oil. ¹H NMR (CDCl₃) δ 5.19 (br d, 1H, *J* = 7.5 Hz), 4.91 (s, 2H), 4.51–4.38 (m, 1H), 4.07–4.27 (m, 2H), 2.93–2.26 (m, 2H), 2.26 (s, 3H), 1.40 (s, 9H), 1.26 (t, 3H, *J* = 7.1 Hz).

4.5. Ethyl (*RS*)-2-[*N*-(*tert*-butyloxycarbonyl)amino]-3-[3-(cyanomethoxy)-5-*tert*-butyl-4-isoxazolyl]propionate (**4b**)

Compound **4b** was prepared as described for **4a** using **3b** (1.0 g, 6.2 mmol), K₂CO₃ (853 mg, 6.2 mmol) and chloroacetonitrile (590 μL, 9.3 mmol) in acetone (100 mL). CC [toluene–EtOAc (9:1)] gave **4b** (983 mg, 86%) as colourless crystals. ¹H NMR (CDCl₃) δ 5.19 (d, 1H, *J* = 8.0 Hz), 4.95 (s, 2H), 4.49 (dd, 1H, *J* = 6.4 and 8.5 Hz), 4.12–4.30 (m, 2H), 2.95 (dd, 1H, *J* = 6.4 and 10.7 Hz), 2.75 (dd, 1H, *J* = 6.4 and 14.7 Hz), 1.38 (s, 18H), 1.23 (t, 3H, *J* = 7.1 Hz).

4.6. Ethyl (*RS*)-2-[*N*-(*tert*-butyloxycarbonyl)amino]-3-[3-(tetrazolylmethoxy)-5-methyl-4-isoxazolyl]propionate (**5a**)

A mixture of **4a** (480 mg, 1.36 mmol) and sodium azide (194 mg, 2.99 mmol) in dry DMF (10 mL) was stirred in a sealed ampoule at 80 °C for 7 days. The reaction mixture was concentrated under reduced pressure, H₂O added (10 mL) and acidified to pH 3 with 2 M HCl. The aqueous phase was extracted with EtO₂ and the organic phase washed with aq. sat. CaCl₂. After drying, evaporation and CC [toluene–EtOAc–AcOH (49:49:2)] followed by recrystallization (EtOAc–light petroleum) gave **5a** (350 mg, 65%) as colourless crystals: mp 140–141 °C. ¹H NMR (CDCl₃) δ 9.18 (br s, 1H), 5.87 (d, 1H, *J* = 14.9 Hz), 5.70 (d, 1H, *J* = 14.9 Hz), 4.95 (s, 2H), 4.49 (dd, 1H, *J* = 6.4 and 8.5 Hz), 4.12–4.30 (m, 2H), 2.95 (dd, 1H, *J* = 6.4 and 10.7 Hz), 2.75 (dd, 1H, *J* = 6.4 and 14.7 Hz), 1.38 (s, 18H), 1.23 (t, 3H, *J* = 7.1 Hz). Elemental analysis (C₁₆H₂₄N₆O₆): calcd 48.44% C, 6.10% H, 21.27% N; found 48.10% C, 6.21% H, 21.27% N.

4.7. Ethyl (*RS*)-2-[*N*-(*tert*-butyloxycarbonyl)amino]-3-[3-(tetrazolylmethoxy)-5-*tert*-butyl-4-isoxazolyl]propionate (**5b**)

A mixture of **4b** (730 mg, 1.84 mmol), sodium azide (232 mg, 3.68 mmol) and TEA hydrochloride (507 mg, 3.68 mmol) in DMF (20 mL) was stirred for 16 h at 90 °C. The reaction mixture was concentrated under reduced pressure, H₂O added (20 mL) and acidified to pH 3 with 2 M HCl. The aqueous phase was extracted with EtO₂ and the organic phase washed with aq. sat. CaCl₂. After drying, evaporation and CC [toluene–EtOAc–AcOH (80:18:2)] gave **5b** (690 mg, 85%) as colourless crystals. ¹H NMR (CDCl₃) δ 5.90 (d, 1H, *J* = 15.0 Hz), 5.71 (d, 1H, *J* = 15.0 Hz), 5.56 (d, 1H, *J* = 8.7 Hz), 4.70–4.83 (m, 1H), 4.11–4.30 (m, 2H), 3.01 (dd, 1H, *J* = 6.7 and 14.7 Hz), 2.87 (dd, 1H, *J* = 8.8 and 14.7 Hz), 1.45 (s, 9H), 1.35 (s, 9H), 1.29 (t, 3H, *J* = 7.0 Hz). Elemental analysis (C₁₉H₃₀N₆O₆): calcd 52.04% C, 6.90% H, 19.17% N; found 52.19% C, 6.94% H, 19.04% N.

4.8. (*RS*)-2-Amino-3-[3-(tetrazolylmethoxy)-5-methyl-4-isoxazolyl]propionic acid Zwitterion (**1a**)

A mixture of **5a** (290 mg, 0.73 mmol) in aqueous TFA (9 mL, 1 M) was refluxed for 24 h. The reaction mixture was evaporated and recrystallization (H₂O) gave **1a** (133 mg, 68%) as colourless crystals: mp 230 °C (decomp.). ¹H NMR (D₂O) δ 5.55 (s, 2H), 4.22 (t, 2H, *J* = 6.1 Hz), 3.01 (d, 2H, *J* = 6.19 Hz), 2.27 (s, 3H). Elemental analysis (C₉H₁₂N₆O₄) calcd 40.25% C, 4.50% H, 31.42% N; found 40.05% C, 4.77% H, 31.12% N.

4.9. (*RS*)-2-Amino-3-[3-(tetrazolylmethoxy)-5-*tert*-butyl-4-isoxazolyl]propionic acid Zwitterion (**1b**)

A mixture of **5b** (480 mg, 1.09 mmol) in aqueous TFA (20 mL, 1 M) was refluxed for 24 h. The reaction mixture was evaporated, H₂O added and pH adjusted to

pH 3 with 1 M NaOH. The solution was evaporated and recrystallization twice (H₂O) gave **1b** (55 mg, 16%) as colourless crystals: mp 210 °C (decomp.). ¹H NMR (D₂O) δ 5.56 (s, 2H), 4.01–3.94 (m, 1H), 3.15–2.87 (m, 2H), 1.19 (s, 9H). Elemental analysis (C₁₂H₁₈N₆O₄) calcd 46.45% C, 5.85% H, 27.08% N; found 46.47% C, 5.72% H, 26.89% N.

5. In vitro pharmacology

5.1. Cell culture and second messenger assays

Chinese hamster ovary (CHO) cell lines expressing mGluR1α, mGluR2 and mGluR4a were maintained as previously described.^{5,29,30} Briefly, cells were maintained in a humidified 5% CO₂/95% air atmosphere at 37 °C in DMEM containing GlutaMAX-I and 10% dialyzed fetal calf serum (all Gibco, Paisly, Scotland). The day before the inositol phosphate assay, two million mGluR1α-expressing cells were divided into the wells of a 96-well plate in inositol-free culture medium containing 4 μCi/mL [³H]inositol. The day before the cyclic AMP assay, two million mGluR2- or mGluR4a-expressing cells were divided into the wells of a 96-well plate in culture medium. Measurements of inositol phosphate generation and cyclic AMP inhibition were determined by ion-exchange chromatography and scintillation proximity assays as previously described.³¹

5.2. Receptor binding assays

The membrane preparations used in receptor binding experiments were prepared according to Ransom and Sec.³² Affinities for AMPA, KA and NMDA receptor sites were determined using the respective ligands [³H]AMPA,³³ [³H]KA,³⁴ [³H]CNQX and [³H]CPP.³⁵ The binding assays were carried out with the modifications previously described.²⁵

5.3. Electrophysiology

Two-electrode voltage-clamp recordings were performed on *X. laevis* oocytes expressing cloned AMPA and KA receptors clamped at –70 to –50 mV. On AMPA receptors, we analyzed inhibition of 25 μM KA, while at GluR5 and heteromeric GluR6/KA2 receptors we recorded inhibition of the current elicited by 10 μM KA and 20 μM AMPA, respectively. Oocytes expressing KA receptors were treated with 1 mg/mL concanavalin A for 5 min prior to recording, to reduce the degree of desensitization (for further details see Ref. 11). All AMPA receptors were of the flop splice variant^{2,36} and homomeric GluR2 receptors were un-edited at the Q/R site.³⁷

5.4. Data analysis

To compensate for possible run-down or run-up of the currents recorded in the two-electrode voltage-clamp setup, we normalized the responses to alternating currents elicited by the agonist applied alone. Data were subsequently fitted to the following equation to

define the IC_{50} values: $I = I_{\max} \times \{ (IC_{50}^{nH}) / (IC_{50}^{nH} + [Anta]^{nH}) \}$, where I is the current elicited at a given antagonist concentration, $[Anta]$. I_{\max} is the current elicited by the agonist without antagonist included in the test solution, and nH is the Hill coefficient of the antagonist. IC_{50} values were later converted to K_b values using the Leff–Dougall equation.³⁸ $K_b = IC_{50} / \{ 2 + ([A]/[A]_{50})^{1/nH} - 1 \}$, where $[A]$ is the concentration of the used agonist, $[A]_{50}$ is the EC_{50} value for the agonist and nH is the Hill coefficient of the agonist. The respective EC_{50} values (and Hill coefficients) were 24(1,3), 130(1,1), 53(1,3), 34(1,1), 9,6(1,4) and 110(1,0) (all EC_{50} values in μM) for the agonists applied at GluR1, GluR2, GluR3, GluR4, GluR5 and GluR6/KA2, respectively (see Ref. 28 and values determined in our laboratory).

6. Computational methods

The experimental crystal structure of the GluR2–S1S2/ATPO complex 1N0T.pdb³⁹ was used as a representative of the antagonized state of AMPA receptors, given the very high degree of conservation of the binding site among GluR1–4. Following the procedure used to model the agonized receptor state of GluR5,²⁴ a model of GluR5/ATPO was produced by comparative modelling with GluR2/DNQX (1FTL.pdb chainA)⁴⁰ and GluR2/ATPO (1N0T.pdb chainB)³¹ using Swissmodel, first approach mode.⁴¹ The GluR5/ATPO model and GluR2/ATPO(chainA) (which is extremely similar to ATPO chainB) were then prepared using Impact2.5,⁴² according to the recommended methods, except that during constrained minimization (impref) the target RMS deviation was set to 1.0 Å. Electrostatic and van der Waals grids were calculated for the binding sites using Glide2.5,⁴² with a 16 Å box and default parameters, except for scaling the van der Waals radii of non-polar atoms by a factor of 0.9. AMOA, ATPO, **1a** and **1b** were minimized and subjected to Monte Carlo conformational analysis using MMFFs⁴³ and GB/SA continuum treatment of aqueous solvation in MacroModel 8.1.⁴² The phosphonates and carboxylates were modelled as monoanions, the α -amino acids as zwitterions, and the tetrazoles as the neutral 1H tautomers (due to lack of appropriate atom types). Following conformational searching, the global minima of the tetrazoles were converted to the corresponding triionized forms, to match the other ligands. All four compounds were then docked to GluR2 and the GluR5 model using Glide2.5,⁴² with default parameters apart from scaling of non-polar atomic radii by 0.9, and retention of the 30 best poses for each ligand. The best poses had Emodel scores of (–144.9, –155.7), (–171.0, –169.0), (–140.1, –141.9) and (–144.3, –137.8) for AMOA, ATPO, **1a** and **1b** at (GluR2, GluR5), respectively.

Acknowledgments

The authors thank the Lundbeck Foundation, the Danish Medicinal Research and the Novo Nordisk Foundation for financial support, and the computing resources

of the Danish Center for Scientific Computing and the Australian Centre for Advanced Computing and Communications.

References and notes

- Parsons, C. G.; Danysz, W.; Quack, G. *Drug News Perspect.* **1998**, *11*, 523–569.
- Monaghan, D. T.; Wenthold, R. J. *The Ionotropic Glutamate Receptors*; Humana Press: Totowa, New Jersey, 1997.
- Wheal, H. V.; Thomson, A. M. *Excitatory Amino Acids and Synaptic Transmission*; Academic Press: London, 1995.
- Bräuner-Osborne, H.; Egebjerg, J.; Nielsen, E. O.; Madsen, U.; Krogsgaard-Larsen, P. *J. Med. Chem.* **2000**, *43*, 2609–2645.
- Tanabe, Y.; Masu, M.; Ishii, T.; Shigemoto, R.; Nakanishi, S. *Neuron* **1992**, *8*, 169–179.
- Madden, D. R. *Nat. Rev. Neurosci.* **2002**, *3*, 91–101.
- Rosenmund, C.; Stern-Bach, Y.; Stevens, C. F. *Science* **1998**, *280*, 1596–1599.
- Dingledine, R.; Borges, K.; Bowie, D.; Traynelis, S. F. *Pharmacol. Rev.* **1999**, *51*, 7–61.
- Krogsgaard-Larsen, P.; Honore, T.; Hansen, J. J.; Curtis, D. R.; Lodge, D. *Nature* **1980**, *284*, 64–66.
- Clarke, V. R.; Ballyk, B. A.; Hoo, K. H.; Mandelzys, A.; Pellizzari, A.; Bath, C. P.; Thomas, J.; Sharpe, E. F.; Davies, C. H.; Ornstein, P. L.; Schoepp, D. D.; Kamboj, R. K.; Collingridge, G. L.; Lodge, D.; Bleakman, D. *Nature* **1997**, *389*, 599–603.
- Nielsen, M. M.; Liljefors, T.; Krogsgaard-Larsen, P.; Egebjerg, J. *Mol. Pharmacol.* **2003**, *63*, 19–25.
- Krogsgaard-Larsen, P.; Ferkany, J. W.; Nielsen, E. Ø.; Madsen, U.; Ebert, B.; Johansen, J. S.; Diemer, N. H.; Bruhn, T.; Beattie, D. T.; Curtis, D. R. *J. Med. Chem.* **1991**, *34*, 123–130.
- Møller, E. H.; Egebjerg, J.; Brehm, L.; Stensbøl, T. B.; Johansen, T. N.; Madsen, U.; Krogsgaard-Larsen, P. *Chirality* **1999**, *11*, 752–759.
- Herr, R. J. *Bioorg. Med. Chem.* **2002**, *10*, 3379–3393.
- Ornstein, P. L.; Arnold, M. B.; Augenstein, N. K.; Lodge, D.; Leander, J. D.; Schoepp, D. D. *J. Med. Chem.* **1993**, *36*, 2046–2048.
- Lunn, W. H. W.; Schoepp, D. D.; Calligaro, D. O.; Vasileff, R. T.; Heinz, L. J.; Salhoff, C. R.; O'Malley, P. J. *J. Med. Chem.* **1992**, *35*, 4608–4612.
- Honoré, T.; Lauridsen, J. *Acta Chem. Scand.* **1980**, *B34*, 235–240.
- Lauridsen, J.; Honoré, T.; Krogsgaard-Larsen, P. *J. Med. Chem.* **1985**, *28*, 668–672.
- Madsen, U.; Bang-Andersen, B.; Brehm, L.; Christensen, I. T.; Ebert, B.; Kristoffersen, I. T. S.; Lang, Y.; Krogsgaard-Larsen, P. *J. Med. Chem.* **1996**, *39*, 1682–1691.
- Harrison, N. L.; Simmonds, M. A. *Br. J. Pharmacol.* **1985**, *84*, 381–391.
- Vogensen, S. B.; Jensen, H. S.; Stensbøl, T. B.; Frydenvang, K.; Bang-Andersen, B.; Johansen, T. N.; Egebjerg, J.; Krogsgaard-Larsen, P. *Chirality* **2000**, *12*, 705–713.
- Krogsgaard-Larsen, P.; Ebert, B.; Lund, T. M.; Bräuner-Osborne, H.; Sløk, F. A.; Johansen, T. N.; Brehm, L.; Madsen, U. *Eur. J. Med. Chem.* **1996**, *31*, 515–537.
- Madsen, U.; Frølund, B.; Lund, T. M.; Ebert, B.; Krogsgaard-Larsen, P. *Eur. J. Med. Chem.* **1993**, *28*, 791–800.
- Brehm, L.; Greenwood, J. R.; Hansen, K. B.; Nielsen, B.; Egebjerg, J.; Stensbøl, T. B.; Bräuner-Osborne, H.; Sløk,

- F. A.; Kronborg, T. T.; Krogsgaard-Larsen, P. *J. Med. Chem.* **2003**, *46*, 1350–1358.
25. Stensbøl, T. B.; Borre, L.; Johansen, T. N.; Egebjerg, J.; Madsen, U.; Ebert, B.; Krogsgaard-Larsen, P. *Eur. J. Pharmacol.* **1999**, *380*, 153–162.
26. Chittajallu, R.; Braithwaite, S. P.; Clarke, V. R.; Henley, J. M. *Trends Pharmacol. Sci.* **1999**, *20*, 26–35.
27. Thomas, N. K.; Hawkins, L. M.; Miller, J. C.; Troop, H. M.; Roberts, P. J.; Jane, D. E. *Neuropharmacology* **1998**, *37*, 1223–1237.
28. Wahl, P.; Anker, C.; Traynelis, S. F.; Egebjerg, J.; Rasmussen, J. S.; Krogsgaard-Larsen, P.; Madsen, U. *Mol. Pharmacol.* **1998**, *53*, 590–596.
29. Tanabe, Y.; Nomura, A.; Masu, M.; Shigemoto, R.; Mizuno, N.; Nakanishi, S. *J. Neurosci.* **1993**, *13*, 1372–1378.
30. Aramori, I.; Nakanishi, S. *Neuron* **1992**, *8*, 757–765.
31. Bräuner-Osborne, H.; Nielsen, B.; Krogsgaard-Larsen, P. *Eur. J. Pharmacol.* **1998**, *350*, 311–316.
32. Ransom, R. W.; Stec, N. L. *J. Neurochem.* **1988**, *51*, 830–836.
33. Honore, T.; Nielsen, M. *Neurosci. Lett.* **1985**, *54*, 27–32.
34. Braitman, D. J.; Coyle, J. T. *Neuropharmacology* **1987**, *26*, 1247–1251.
35. Murphy, D. E.; Schneider, J.; Boehm, C.; Lehmann, J.; Williams, K. *J. Pharmacol. Exp. Ther.* **1987**, *240*, 778–783.
36. Sommer, B.; Keinänen, K.; Verdoorn, T. A.; Wisden, W.; Burnashev, N.; Herb, A.; Köhler, M.; Takagi, T.; Sakmann, B.; Seeburg, P. H. *Science* **1990**, *249*, 1580–1585.
37. Sommer, B.; Kohler, M.; Sprengel, R.; Seeburg, P. H. *Cell* **1991**, *67*, 11–19.
38. Leff, P.; Dougall, I. G. *Trends Pharmacol. Sci.* **1993**, *14*, 110–112.
39. Hogner, A.; Kastrup, J. S.; Jin, R.; Liljefors, T.; Mayer, M. L.; Egebjerg, J.; Larsen, I. K.; Gouaux, E. *J. Mol. Biol.* **2002**, *322*, 93–109.
40. Armstrong, N.; Gouaux, E. *Neuron* **2000**, *28*, 165–181.
41. Schwede, T.; Diemand, A.; Guex, N.; Peitsch, M. C. *Res. Microbiol.* **2000**, *151*, 107–112.
42. Schrödinger, I. 1500 S.W. First Avenue, Suite 1180 Portland, OR 97201, USA, 2003.
43. Halgren, T. A. *J. Comput. Chem.* **1999**, *20*, 730–748.